Energy and Buildings 155 (2017) 378–389

Contents lists available at ScienceDirect

Energy and Buildings

journal homepage: www.elsevier.com/locate/enbuild

Replication Studies

A ventilation system controller based on pressure-drop and CO_2 models

Gerhard Zucker[a,*], Andreas Sporr[a], Antonio Garrido-Marijuan[a], Tarik Ferhatbegovic[a], René Hofmann[a,b]

[a] AIT Austrian Institute of Technology, Center for Energy, Donau-City-Straße 1, 1220 Vienna, Austria
[b] TU Wien, Institute for Energy Systems and Thermodynamics, Getreidemarkt 9/302, 1060 Vienna, Austria

ARTICLE INFO

Article history:
Received 28 April 2017
Received in revised form 31 July 2017
Accepted 15 September 2017
Available online 18 September 2017

Keywords:
Ventilation system
Pressure-drop model
Ventilation controller
Volume flow optimization

ABSTRACT

In ventilation systems a considerable amount of energy is used for mass transport of conditioned air to provide the requested volume flows. Reducing volume flow while maintaining indoor air quality has leverage on energy efficiency and is commonly known as Demand Controlled Ventilation (DCV). Current implementations require Variable Air Volume (VAV) controllers to provide a defined volume flow to each room. The controllers measure the pressure difference and adjust the motor flap accordingly. This paper examines an approach that achieves DCV, but replaces the VAV-boxes with simple motor flaps. The missing pressure-drop measurements that allow calculating the volume flow are substituted by a model of the ventilation system. The authors develop a method for calculating the pressure drop in the ducts of a ventilation system that regards the topology and the components of the duct system. This model is coupled with a model for the CO_2 concentration in the rooms for all conditioned rooms in order to derive the required air volume flow. Using this model, a linear controller is developed that operates the ventilation system. It is shown that the presented approach operates the ventilation more efficiently, while maintaining comfort constraints and saving installation costs. The modeling effort of the current approach is expected to be reduced with the introduction of the Building Information Model (BIM) into building operation.

1. Introduction

Energy consumption in buildings represents 40% of the final energy demand in Europe – and they consume more energy than any other sector of the European economy [1]. About half of the energy consumed in building operation is invested into heating, ventilation and air conditioning (HVAC) [2], whereby in the US ventilation represents about 61% of the total electric power consumption in office HVAC systems [3]. In many modern buildings the air conditioning system does not contribute significantly to heating or cooling, but shall rather condition the indoor air to be at the right level of CO_2 and within the comfort zone in the Mollier-h-x diagram. In this work, the authors therefore focus on energy optimizations based on volume flow reductions and disregard the energy needed for heating or cooling the air as well as the energy for adjusting the humidity – based on the valid assumption that reduced volume flow will in parallel also save energy for heating, cooling, humidification and dehumidification.

At the same time, buildings need to balance between maximum energy efficiency and optimal indoor air composition and quality (IACQ). IACQ has gained great importance due to the significant increment of illnesses reported by building occupants, referred as sick building syndrome (SBS) [4,5]. Z. Lin et al. [6] suggest that multiple factors are involved in this syndrome, including indoor air quality (IAQ) such as microbiological and chemical exposures not adequately characterized by current assessment approaches. This study also shows that with proper design, installation, maintenance and operation, the ventilation mechanisms of buildings can maintain satisfactory levels of IAQ and therefore reduce the SBB incidence. Today there is no real integration of IACQ and energy efficiency, being mainly the domains of different communities working independently. Different studies [7,8] have shown that some energy efficient buildings reduce the conventional energy consumption by means of reducing volume flow with a number of ventilations below the standards, and therefore a reduction on IACQ. By observing how HVAC designers commonly address the above 40% of energy use for space heating and cooling, it is found

* Corresponding author.
E-mail address: gerhard.zucker@ait.ac.at (G. Zucker).

http://dx.doi.org/10.1016/j.enbuild.2017.09.041
0378-7788/

Nomenclature

Abbreviations

CSP	Constant static pressure
DCV	Demand controlled ventilation
HVAC	Heating ventilation and air conditioning
IACQ	Indoor air composition and quality
NOAA	National oceanic and atmospheric administration
SPR	Set-point reset
VAV	Variable air volume

Latin Symbols

a [-]	Constant
b [-]	Constant
A [m^2]	Cross section of the duct
$\dot{C}_{Co2}$ [ppm/s]	CO_2 production per hour of the persons
C [ppm]	CO_2 level
d [m]	Duct diameter
l [m]	Duct length
L [Pa s^2/m^3]	Hydraulic inductance
n [1/h]	Air change rate through windows and the ventilation system
p [Pa]	Pressure
R [Ω]	Electric resistance
R [J/(kgK)]	Specific gas constant
Re [–]	Reynolds number
$\dot{V}$ [m^3/h]	Volume flow

Greek Symbols

α [deg]	Flap angle
Δ [1]	Difference
λ [m]	Friction factor
ρ [kg/m^3]	Density
ϑ [m/s]	Velocity
υ [m^2/s]	Kinematic viscosity
ς [-]	Pressure drop coefficient

Indices

a	Outside
i	Inside
w	Window

out that the design focuses on minimizing energy use/cost, which often leads to unhealthy indoor comfort conditions.

2. Motivation and technical concept

Providing indoor air quality and minimizing the energy demand for the ventilation system are contradictory goals. An optimization needs to be well-designed in order to provide the same, if not better, services than conventional buildings and to reach the same comfort parameters and indoor air quality. The main electric consumers are the fans in the duct system, namely the supply air fans and exhaust air fans. Therefore the first motivation is to find an appropriate control strategy for controlling the fans. Volume flow and pressure have a quadratic relation, volume flow and power consumption have a cubic relation as shown in Fig. 1. A reduction of the volume flow by 10% results in an electric power reduction of 27%, thus giving a significant leverage for energy savings. This both applies to reduction of the overall volume flow that is required to meet the comfort criteria, but also to avoiding periods of high volume flow followed by periods of low volume flow, if it is possible to level out these periods to an average volume flow. An energy efficient control strategy for a given ventilation system shall attempt to keep the volume flow

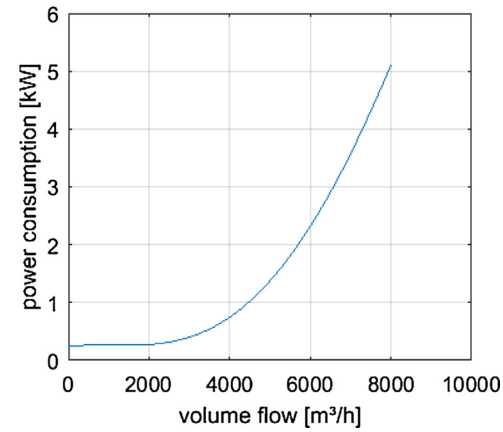

Fig. 1. Cubic relation between power consumption over volume flow for a Robatherm RMC 06/12 fan.

as low as possible, as seen in Fig. 1, while maintaining the indoor comfort.

The second motivation is to exploit the designed systems for reducing costs. While the operation costs are automatically reduced by the targeted optimization of volume flows (which reduces consumption of electric energy, of thermal energy due to reduced volumes that need to be conditioned and of maintenance costs due to reduced stress on the mechanical fans), the installation costs are not addressed. In order to also reduce investments when constructing the building, expensive components can be replaced. In the case of ventilation systems, these are the VAV boxes. In principle, the VAV boxes can be replaced by motor flaps, which are also able to adapt the volume flow for each room, but lack the additional sensory equipment to measure the volume flow: a VAV controller can maintain a given volume flow set-point, so the volume flow into the room is known. A motor flap can only control the flap position to open and close between 0% and 100%. The volume flow, however, is unknown, since it depends not only on the flap position, but also on the current pressure in the duct system. By introducing a model for the motor flap that contains the dependencies of flap angle, pressure and volume flow, we can use the flap model to derive the volume flow, given that the pressure in the duct system is known. This way the construction costs for the building are reduced in both hardware costs and installation costs by performing a shift from hardware to control design and plant modeling.

Analysis of indoor air quality issues in national regulations are commonly addressed by measurement of CO_2 levels, based on its association with human body odor and other pollutants [9], not with any health or comfort effects of CO_2 itself. This approach relies on the fact that CO_2 detection technologies are well established and it is common knowledge that this technology provides quite good indicators of IACQ, which in turn are used for operating the building ventilation system.

This paper is organized as follows: Section 3 discusses the existing state of the art in control strategies for ventilation systems, Section 4 describes the models that are needed for the design of the new control strategy, which is then described in Section 5. The results are presented in Section 6, followed by the Conclusions in Section 7.

3. State of the art

Fig. 2 shows the control scheme of a CO_2 room control: the linear PID-controller *Control* maintains the CO_2 level in a room, it receives the difference between the CO_2 set-point and the current CO_2 sensor value; its controlled variable is the volume flow $\dot{V}$. The VAV box modulates an internal flap (using the flap angle α) to deliver

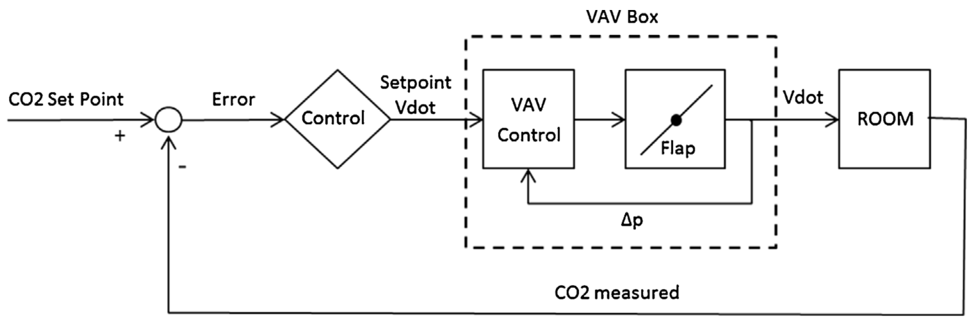

Fig. 2. Ventilation model and room models of the controlled plant.

the requested volume flow, the internal controller *VAV Control* uses the pressure difference Δp to operate the flap, resulting in the volume flow reaching the room and affecting the CO_2 level in the room (a modified control strategy shall achieve the same, but without the internal VAV controller, solely operating on the flap angle).

In a ventilation system the pressure set-point of the fans is often fixed and does not regard the current demand situation. This control strategy is referred to as Constant Static Pressure (CSP) [7]. It is commonly used, due to its simplicity and its low costs: CSP does not require communication between the supply air fan and the VAV controllers, thus saving equipment and installation costs. Consequently, fan control and room control cannot cooperate; this implies that the supply air fan provides a pressure in the ducts of the system, which may be too high for the current demand. The excess pressure in the duct system is compensated by the VAV controllers at the room inlet by closing their flap and reducing the aperture in order to compensate for the high pressure. In CSP, the pressure of the fan is calculated once (usually during commissioning) for one specific occupancy scheme and is scarcely adapted during operation. CSP has two significant disadvantages: firstly it runs the risk of violating the comfort zone by providing low IACQ, if the fan pressure is too low; secondly it may suffer from excessive energy demand due to an over-pressured duct system. Static Pressure Set-point Reset (SPR) [8] is a control strategy that addresses these disadvantages: it allows reducing the fan pressure set-point based on the required volume flow. SPR requires VAV controllers in each room, which have to communicate with the fan controller. The pressure is reduced until at least one VAV box is fully open (i. e. the flap that is controlled by the VAV controller, respectively). At this point any further reduction in pressure would cause too low volume flow in the room. Then the pressure is slightly increased again. This is necessary to detect, if a VAV box needs to open beyond 100%. SPR needs to have a relaxed timing regarding the modification of the pressure in order to avoid oscillations between fan control and VAV controller reaction. Thus the VAV boxes cannot react on fast occupancy (e.g. beginning of a lecture) changes, which can cause violations of the comfort. SPR is used in different VAV controller types like the Belimo VAV compact controller [10] and other controllers.

In [11] the authors extend the SPR approach and suggest a CO_2-based and occupancy-sensor-based dynamic reset of volume flow for multiple zone HVAC systems and indicate cost savings due to reduced outdoor volume flow. The system still depends on controlled volume flow by VAV controllers. The impossibility of setting an accurate volume flow by motor flaps, does not allow a replacement by them. The Trim-and-Respond control strategy [8] is similar to SPR in that it attempts to reduce the volume flow and save energy; it differs in implementation by "trimming" the pressure set-point until a supplied room or zone issues a request that it needs more pressure to fulfil its requirements for IACQ. While trimming has slow dynamics, the requests for more pressure are rapidly executed in order to stay within air quality constraints.

4. Plant modeling

The schematic in Fig. 3 shows a topological model of the plant that shall be controlled. The supply air fan receives a set-point for the differential pressure that it shall provide to the duct system. The volume flow into the different rooms is controlled either by setting a set-point for the volume flow in a VAV controller or by setting the flap angle of a motor flap. Each room is equipped with a CO_2 sensor that provides the current CO_2 concentration (CO_2 level).

The model follows an application oriented design, since it shall be applicable to building energy management applications. Therefore the model uses only available data from sensors and actuators that are commonly installed in a ventilation system and are accessible by the supervisory control system. It does not require additional invasive sensor placement in the duct system. Therefore, the pressure in different segments of the duct system cannot be measured, but is calculated using schematics of the duct system as shown in Section 4.1.

The duct system (including the supply air fan) and the CO_2 models for the rooms are the foundation for the controller design that is covered in detail in Section 5. The duct system model is a *pressure drop model*, which derives the pressure drops for all paths between supply air fan and room supply outlets as well as the volume flow in each segment. The relation between volume flow and CO_2 level is calculated in the CO_2 room models, which assumes that supply volume flow and exhaust volume flow are the same, thus only the supply side is modelled, and the exhaust fan is operated identically to the supply fan.

Fig. 4 shows the dependencies of the sensors and actuators in the system: The supply air fan receives a set-point. While it tries to reach this set-point, it passes the current pressure to the duct system model in the dynamic calculation. Afterwards the VAV boxes receive their volume flow (or their flap angle set-points, respectively) and the current volume flows from the duct system model. The dotted line indicates that all of the VAV boxes/CO_2 room models receive their different set-points and pass on their current volume flows.

The following sections elaborate the details on the models for the duct system (Section 4.1), the pressure characteristics of the VAV controllers and motor flaps (Section 4.2) and the model for the CO_2 concentration in the rooms.

4.1. Modeling the duct system

The pressure drop model of the duct system calculates the current volume flow into the rooms at any moment. This model is based on the pressure drop of the ducts and reflects the topology of the duct system. According to [12] and [13] the pressure drop Δp in a duct segment is calculated as:

$$\Delta p = \lambda \frac{l}{d} \frac{\rho}{2} \vartheta^2 \tag{1}$$

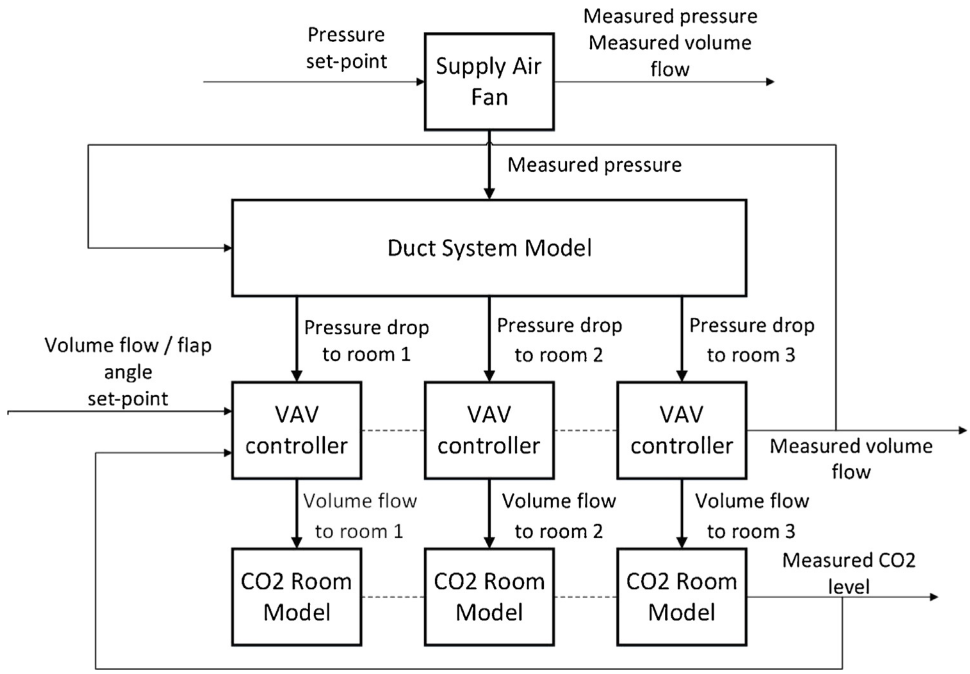

Fig. 3. Ventilation model and room models of the controlled plant.

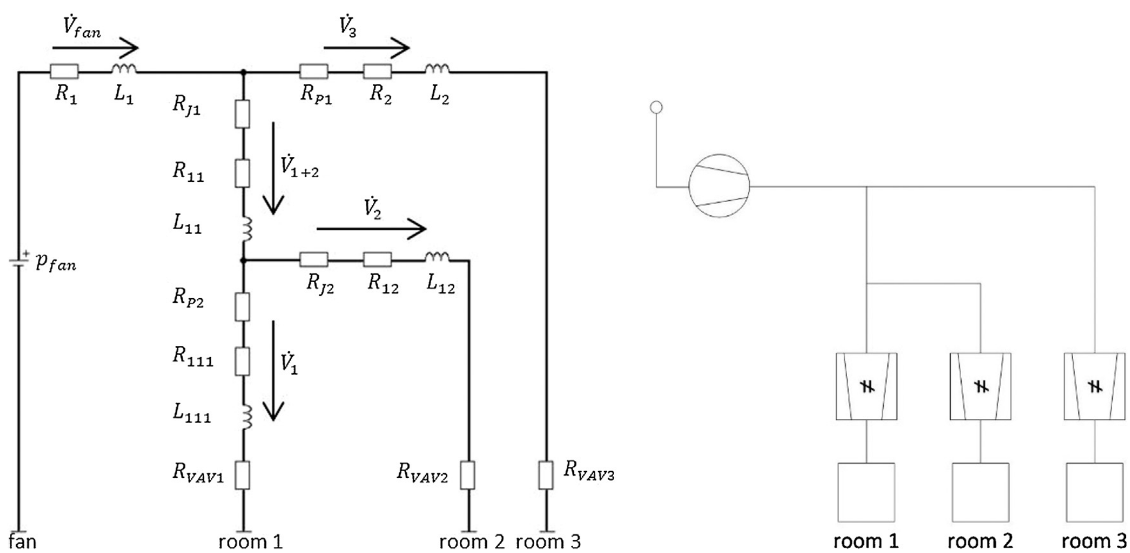

Fig. 4. Electrical substitute circuit diagram (left) for a ventilation system with three rooms (right).

$$\Delta p = \varsigma \frac{\rho}{2} \vartheta^2 \tag{2}$$

In Eq. (1), l is the length of the duct segment, d the diameter, ρ the density of the supply air and in both equations ϑ is the air velocity. For each straight duct segment Eq. (1) can be used, with λ being the friction factor [13–16], which describes the friction losses in pipe flow, depending on the Reynolds number (Eq. (4)) as well as on the roughness and on the diameter of the duct. The pressure drop of special duct types (bifurcations, elbow ducts and other non-straight ducts) can be calculated using Eq. (2), where ς is a coefficient that depends on the shape of the duct and can be found in well-known literature [12,17]. An important conversion is the relation between volume flow and velocity as

$$\vartheta = \frac{\dot{V}}{A} = \frac{1}{A} \frac{dV}{dt} \tag{3}$$

since the sensor readings in the building automation system provide volume flows. The flow's Reynolds number Re is defined as

$$Re = \frac{\vartheta d}{\upsilon} \tag{4}$$

with υ being the kinematic viscosity of the supply air. The dynamics of the duct system can be modelled using the electric analogy of an inductance. The hydraulic (or pneumatic) *inductance* accordingly stores kinetic energy of the volume flow and consequently prohibits instant changes of the volume flow (which is the electric current in the analogy). It reflects the dynamics in the pressure drop model and allows solving it for the different volume flows. The hydraulic inductance L for a duct segment is used in the pressure drop equation as:

$$\Delta p = L\ddot{V} = L\frac{d^2V}{dt^2} \text{ with } L = \frac{l\rho}{A} \tag{5}$$

Using the dynamics of the ducts, a dynamic simulation can be used to calculate the controller coefficients (see Section 5). The duct topology in the building has to be compiled using a combination of duct segments, each causing a certain pressure drop. As a start the building schematics and the floorplan can be used to estimate the number of supply inlets and exhausts. However, the schematics typically reflect only the as-planned state, but not the as-built state; therefore there should be a visual inspection of the duct system to verify the topology and the components that were used. Since the pressure drop is not overly sensitive on the length of segments, as the pressure drop per meter ducts is low, the focus of the visual inspection is on the installation location and completeness of the different pipe parts and components like dampers and bifurcations. Also, any possible leakages shall be recorded to improve the reliability of the model.

After the definition of the different pipe paths, the static and dynamic pressure calculations have to be combined. This is done in the electric analogy using the electric current I as volume flow $\dot{V}$, the resistance R as $\lambda \frac{l}{d} \frac{\rho}{2A^2}$ (or $\varsigma \frac{\rho}{2A^2}$, respectively) and the inductance L as $\frac{l\rho}{A}$. Note that in the hydraulic system the volume flow $\dot{V}$ has a squared ratio to the pressure drop instead of a linear one like the current to the voltage.

The following example is developed for three rooms (Fig. 4). It is simplified just to show the coherence between the different volume flows in these rooms.

Using Kirchhoff's second law we can derive the following formulas:

$$p_{fan} = R_1\dot{V}_{fan}^2 + L_1\ddot{V}_{fan} + (R_{P1} + R_2 + R_{VAV3})\dot{V}_3^2 + L_2\ddot{V}_3 \tag{6}$$

$$(R_{P2} + R_{111} + R_{VAV1})\dot{V}_1^2 + L_{111}\ddot{V}_1 = \left(R_{J2} + R_{12} + R_{VAV2}\right)\dot{V}_2^2 + L_{12}\ddot{V}_2 \tag{7}$$

$$\left(R_{J2} + R_{12} + R_{VAV2}\right)\dot{V}_2^2 + L_{12}\ddot{V}_2 + \left(R_{J1} + R_{11}\right)\left(\dot{V}_1 + \dot{V}_2\right)^2 + L_{11}\left(\ddot{V}_1 + \ddot{V}_2\right) = (R_{P1} + R_2 + R_{VAV3})\dot{V}_3^2 + L_2\ddot{V}_3 \tag{8}$$

The size of the set of formulas increases with the number of rooms and duct segments. In order to visualize the dynamics of the system and to have a test-bed for the controller, the system is simulated in a time-continuous simulation tool, for which the authors chose Simulink. To do so the differential equation system need to be solved for $\ddot{V}_1$, $\ddot{V}_2$, $\ddot{V}_3$ and simulated using an S-function[1] for the system. The resistance of a VAV box is calculated using the characteristics taken from literature, as explained above. Its main parameter is the opening angle of the internal flap, which is also the main actuator for the control system.

There are some parameters, which need to be calculated every time-step, for example the hydraulic resistance R. This value is calculated by using the parameter Reynolds number, which depends on the current volume-flow $\dot{V}$ (and on the roughness and duct diameter, which are both constants). For the calculation, the volume-flow from the previous simulation step is used, which leads to a small simulation error. Within the time period in which the controller is tested, the amount of error is irrelevant and thus can be neglected. During "real-time" operation the controller frequently obtains new volume flow values from the VAV boxes, which eliminates aggregation of errors over time.

After validating the model it is possible to replace the model of the VAV box with a motor flap model. For this case the model is redefined as a static one and the dynamic parts (i. e. the change in volume flow $\ddot{V}$) are deleted, looking only at a static pressure drop model. In a realistic operation environment this is a valid assumption, since the control does not require continuous strong changes, but rather remains on a static set-point. Then the total pressure drop between supply fan and each room is calculated, except for the flap pressure drop. The pressure, which needs to drop at the flap, is the difference between this calculated pressure drop and the provided fan pressure. By using reference data, the controller can calculate backwards, which opening angle is needed. Occurring model inaccuracies will be compensated by the controller once it is operating on the real plant (i.e. the ventilation system). The controller uses the difference between the CO_2-set-point and the current CO_2-value for calculating the required volume flow. Afterwards it uses the abovementioned dependence between opening angle and volume flow to calculate the needed angle, if the equations are solved for R_{VAV1}, R_{VAV2}, R_{VAV3}.

4.2. Motor flap and VAV-box characteristics

One of the most common flaps are so-called Butterfly flaps. They have a moveable part in the middle of the duct, which can be controlled to adapt the volume flow for different pressure conditions. There are different ways to calculate the pressure drop of these flaps: preferably the manufacturer publishes a datasheet, which includes the characteristics for pressure drop depending on the volume flow. If this is not the case, literature provides measurements and equations to calculate the required characteristics [17–19]. VAV-boxes are similar in design and can therefore be modelled the same way. As opposed to VAV boxes, a motor flap does not measure the pressure and thus cannot derive the current volume flow. VAV controllers usually work with pressure drop calculations. They measure the pressure before and after the motor flap. It is possible to calculate the velocity and consequently the volume flow. It is possible to calculate the velocity, as seen in Eq. (3), and consequently the volume flow depending on the Bernoulli-equation:

$$\mathrm{p} + \frac{\rho}{2\vartheta^2} = \text{const.} \tag{9}$$

If the measurement happens at a location where the air is unimpeded, we can convert the equation to

$$p_{before} = p_{after} + \frac{\rho}{2\vartheta^2} \tag{10}$$

and in the following to

$$\vartheta = \sqrt{\frac{2\left(\mathrm{p_{before}} - \mathrm{p_{after}}\right)}{\rho}} \tag{11}$$

By simplifying $p_{before} - p_{after}$ to Δp and assuming $\rho = 1,19^{kg}/_{m^3}$ (for air with a temperature at T=293 K) it is possible to calculate the velocity. The assumption is valid as shown in Fig. 5, since the density of air barely changes at constant temperature in the pressure ranges that are relevant for ventilation systems (up to 500 Pa).

A temperature change would have a bigger influence to the density ρ depending on the converted formula of ideal gases

$$\rho = \frac{p}{RT}, \tag{12}$$

[1] A description of a Simulink block written in C, C++ or Fortran that is compiled and allows interacting with the Simulink engine in a programming language other than Simulink.

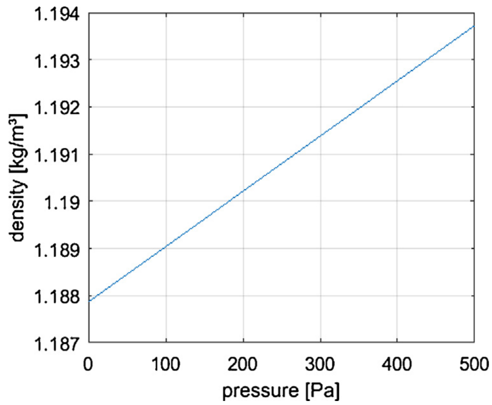

Fig. 5. Ratio between density and pressure.

with the specific gas constant $R = 287, 058\mathrm{J}/(\mathrm{kg\,K})$ and the temperature T.

Due to additional sensory and communication equipment, a VAV-box is more expensive than a motor flap. Therefore it is possible to reduce the costs of a ventilation system by replacing VAV-boxes with motor flaps. The implication is that the volume flow at the VAV outlet is no longer known and therefore cannot be used for control purposes. The approach presented in this paper fills the gap of missing sensory equipment by using the pressure drop model of the duct system to derive the according volume flow into each room, which is done by calculating the pressure drop from the fan to the rooms as shown in Section 4.1.

4.3. Room model for CO_2 concentration

The previous sections defined the plant under control up to the inlet into the room. To complete the plant, it is necessary to model the CO_2 level in a room depending on the incoming volume flow. This is done under the assumption that supply and exhaust volume flow are identical, since there are no significant pressure changes in the building. The CO_2 room model needs to be initialized with the basic room geometry to derive the total air volume. Every room is assumed to have 395 ppm CO_2 as a typical outside air concentration at the beginning of the simulation.

The CO_2 room model is used for controls and therefore is subject to the following simplifications:

- The CO_2 level of the room is stable. That means that the gas doesn't coalesce with other gases.
- CO_2 doesn't adhere at any furnishings, walls, etc.
- The CO_2 level is evenly distributed throughout the room, i. e. the room is a well-mixed and mechanically-ventilated space

Since a controller cannot change the physical setup of the air supply system, it can only attempt to control the plant using the given sensor information. It is therefore assumed that the design of the ventilation system and the sensor placement ensures that with the given equipment the air quality can be maintained throughout the room.

The simplifications allow to calculate with a zero-dimensional mass balance using CO_2 sources and sinks. The only source is the number of persons in the room. Sinks are given by the exchange with outside air through windows and the volume flow of the ventilation system. The resulting mass balance is:

$$V\frac{\partial C_i}{\partial t} = \dot{C}_{Co2} + (C_a - C_i)\,nV \qquad (13)$$

Table 1
Air exchange rates for windows.

Window position	Air exchange rate [1/h]
closed, class 3	0,2–0,4
closed, class 2	0,5–0,8
Tilted	3–10
opened	10–20

Table 2
Tidal volume of people depending on the age and the activity.

Age [Years]	Rest [l/h]	Less activity [l/h]	Average activity [l/h]	Intensive activity [l/h]
>14	22	43	85	152

V is the air volume of the room, $\dot{C}_{Co2}$ the CO_2 production per hour of the persons, C_a the outside CO_2 level, C_i the inside CO_2 level and n the air change rate through windows and the ventilation system.

The air exchange rate is calculated by

$$n = n_W + \frac{\dot{V}}{V} \qquad (14)$$

The air exchange rate for windows n_W is estimated as shown in Table 1. These values represent a summary from standards and literature that were surveyed [20–23].

The exchange rate depending on the volume flow $\dot{V}$ is based on the ratio between the volume flow into the room and the total one of the room. The current CO_2 level, which is needed for the calculation, was taken from the National Oceanic and Atmospheric Administration (NOAA), [24].

Every person produces about 4000 ppm CO_2 per breath in rest [25], the amount of exhaled air depends on age and the activity and can be estimated according to Table 2. Thus it is possible to approximate the concentration change rate $\dot{C}_{Co2}$ given that the number of people in the room is known and derive the current CO_2 level. The number of people may be derived from mechanisms such as people counters, calendars in case of meeting rooms or lectures timetables in case of universities. Based on these variables, it is possible to predict the indoor air quality at time step t and calculate the optimal volume flow needed to maintain the CO_2 level for every room. Since the number of persons, the activities and the window air exchange rate are only estimates, the calculation is valid only with a certain confidence. However, the ventilation system is operated in a closed control loop, which tolerates plant-model mismatches and uses the controller design shown in Section 5 to compensate the model errors.

5. Controller design

Conventional ventilation control strategies set a constant pressure difference at the supply air fan and control the CO_2 level using the volume flow controllers. The volume flow controller closes the motor flap in order to provide the required amount of volume flow to a room. In situations with low volume flow demand, most of the volume flow controllers may be closed, thus creating a high pressure drop at the motor flaps. The supply air fan then has to work against this pressure drop, although the pressure is not necessary, which results in unnecessary electricity demand for the fan. As shown in Section 3, SPR, Trim-and-Respond and other extended control strategies address this problem, but require costly volume flow controllers. The control design in this work approaches the problem by utilizing the plant models for duct system, flaps and CO_2-level in order to improve energy efficiency and air quality and at the same time make way for an implementation with reduced component and installation costs by replacing volume flow controllers with motor flaps.

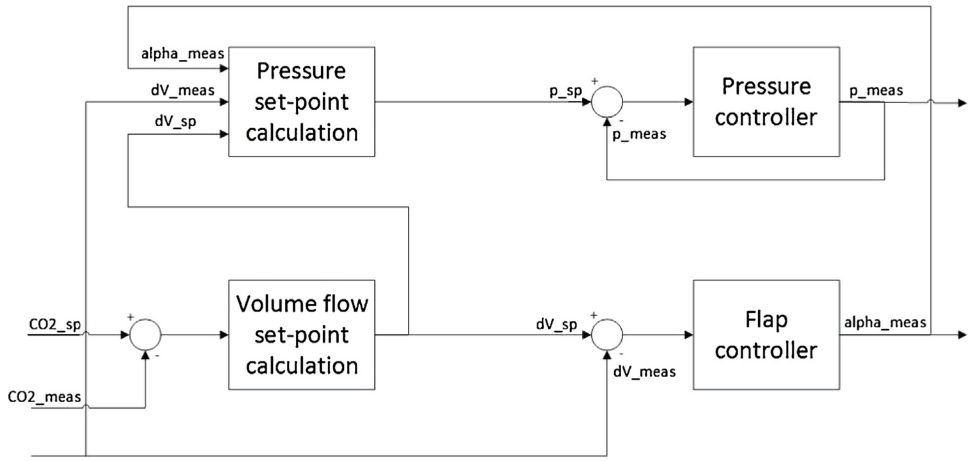

Fig. 6. Schematic of the ventilation controller.

For a given building it is first of all necessary to design and parameterize the pressure drop model of the duct system and the CO_2 models of the rooms. Reference values for average volume flows are taken from literature (see Section 4). For a given volume flow set-point it is then possible to calculate the pressure drop in the duct system from the supply fan to the room outlet of each room (see Section 4.1). This is done for each path from fan to every room outlet, resulting in a list of pressure drops. The highest of these pressure drops defines the maximum pressure the fan has to provide, and it will then provide the sum of all volume flows that the VAVs request. This means that one of the VAV controllers will have its flap fully open (the one with the highest pressure drop), while the other VAVs will react to the given pressure drop by closing their flap so that the requested amount of volume flow is provided for the according room. This procedure is similar to the SPR and Trim-and-Respond strategies. However, if the characteristics of the flap are added to the plant model, the VAV boxes can be replaced with motor flaps as argued in Section 2, without affecting the controller design structure.

The approach depends on the knowledge of the volume flow set-points for each room, these are derived using the CO_2 room model and an estimated occupancy, which can be taken from a room booking schedule or from the design values for room occupancy. The volume flow set-point for each room is calculated by means of a linear PI-controller that uses the current CO_2 levels and the CO_2 set-points as inputs.

There is an additional caveat that the ventilation controller has to regard: the first is that the calculated volume flow will most likely not be sufficient for supply. A real-world ventilation system is not airtight and may have suffered leaks during construction or due to aging (e.g. installation faults causing leakages). Similarly, the demonstration system (Section 6.1) showed to contain outlets without controlled airflow, which results in losses of volume flow that is unknown, since it could only be measured with significant effort. This implies that the controller has to provide more volume flow than the model calculations require. Due to the nature of building design, these factors cannot and shall not be measured (for cost reasons), therefore the controller design has to foresee a safety margin to ensure proper air supply.

Fig. 6 shows the controller schematic with the measured values (suffix *_meas*) and the set-points (suffix *_sp*). The calculations described above are located in the *Pressure set-point* calculation and the Volume *flow set-point calculation* block. Necessary (measured) input values are the CO_2 level CO_2, the volume flow *dV*, the pressure *p* and the flap position (or flap angle, respectively) α (*alpha*).

In a first step the necessary set-points are calculated: the pressure set-point uses the pressure drop calculation of the duct system as shown in Section 4.1. The result is the identification of the highest pressure drop and therefore the needed fan pressure. The volume-flow set-point calculation is based on the CO_2 room model described in Section 4.3, using the CO_2 production and air exchange to derive the needed volume. The calculated set-points are the inputs for the *Pressure controller* and the *Flap controller*, respectively. The pressure controller is configured using the measurement data that identifies the fan characteristics i. e. the correlation between pressure, volume flow and rotational speed. The flap controller is actually a set of PID-controllers, one for each room that is controlled by a VAV controller or by directly controlling the motor flaps.

6. Validation and results

The presented approach consists of models for the ventilation system and its components, the CO_2 room model and the newly developed ventilation controller. The validation of the complete approach focuses on an existing demonstration system that is used as a data source for operation data and as a template for the controller design. The most critical control actuator, the motor flap inside the VAV box (or as a stand-alone component), is validated separately using the recorded operation data. Finally, the newly designed controller is compared against an advance state-of-the-art controller.

6.1. Demonstration system

The ventilation system, which is used to validate the models supplies lecture halls, IT labs, seminar rooms, offices and the corridors on two floors in a passive house office building in Vienna, Austria. The provisioning system consists of the supply air fan, a heating and a cooling register. The differential pressure is measured downstream of the heating register; therefore the pressure drops in the provisioning components are not relevant, since the supply air fan controller maintains the pressure difference between outside air pressure and the measurement downstream of the provisioning system.

The volume flow into the entrance hall and the offices is fixed by one constant volume flow controller with a volume flow set-point of 580 m^3/h for the entrance hall and a second controller with a set-point of 600 m^3/h for the volume flow for all offices. The volume flow into the corridors is neither controlled nor measured, which is a common design decision based on lower costs for simple mechanical outlets in the corridors. The IT labs, lecture halls and seminar rooms are equipped with Variable Air Volume (VAV) controllers that receive set-points for volume flows from the building management system. The VAV controllers do not communicate between each other or the supply fan. In the scope of this paper a subset of the demonstration system with a topology shown in Fig. 4 provides the data needed for plant modeling (see Section 6.4 for the detailed parameter specification). In the following sections the pressure drop model of the ventilation ducts and the motor flaps are the key components that have to be validated.

6.2. Validation of pressure drop model

The pressure drop model of the ventilation duct system that is described in Section 4.1 has to be validated by comparing the model data with experimental data, this is, against the behavior of the demonstration system under real conditions of use. The recorded operation data includes the current volume flow into each room, the volume flow set-point for each room, the volume flow of the supply fan and the provided pressure of the supply fan. In a first step the pressure drop model for the duct system was created, using the available schematics to determine duct diameter, shape, length and geometry (including 90° turn, bifurcation and other geometries that affect the friction in the ducts). This model reflects the as-planned state of the duct topology and was implemented in MATLAB^{TM}.

The pressure drop model receives the measured volume flow into each room as input data. As an output, the model calculates all pressure drops for all segments in the duct topology and allows to determine the pressure drop between supply fan and every room outlet, including the total pressure drop that is needed to properly provide the required volume flows. Fig. 7 shows the procedure for comparison and validation between the total differential pressure from the measured system and the calculated pressures for every room.

Fig. 8 shows the recorded operation data. The purple line shows the differential pressure directly at the fan i.e. the intensity how much the fan pressurizes the duct system. The other lines show the output of the pressure drop model including the flap model. The validation procedure shows relative good agreement to the measured total differential pressure. While ideally measurements and simulation should match perfectly, this would require significant efforts in measuring the duct system, providing differential

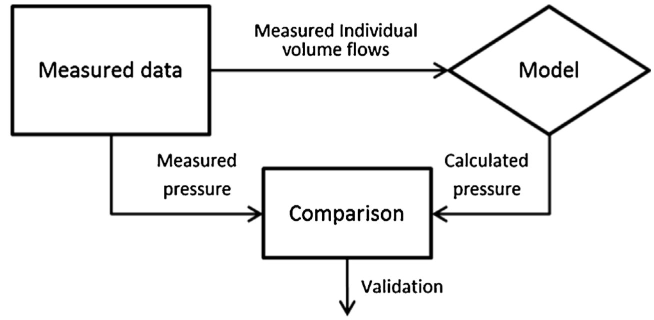

Fig. 7. Validation of the pressure drop model.

pressure sensors at the essential parts of the ventilation system, which could not be argued cost-wise. The model returns confident results about the pressure in the duct system that can be used in a real world environment. Possible violations of the comfort zone by reason of potential plant-model mismatches can be compensated by the closed-loop controller. This kind of controller feedbacks the current CO_2 level, compares it with the CO_2 set-point and tries to compensate this difference.

6.3. Flap identification

In a ventilation system the motor flap located at the room inlet is the main actuator for controlling the volume flow into a room. Using a given pressure in the duct system it is the task of the flap to reduce this pressure so that the required volume enters the room. The remaining pressure difference is taken by the flap. As shown earlier, an efficient controller shall keep this pressure difference low, in order to operate energy efficiently. Modeling of the characteristics is a crucial part for both VAV controllers and direct flap control. However, as the flap opening is usually not known, since it is not recorded by the building automation system which controls the ventilation system. Therefore, other methods have to be investigated to fulfil the requirements for the overall modeling quality. Therefore, the VAV box (or the flap inside the VAV box, respectively) characteristics are described on the basis of three major parameters, which are the (actual) volume flow rate through the VAV box

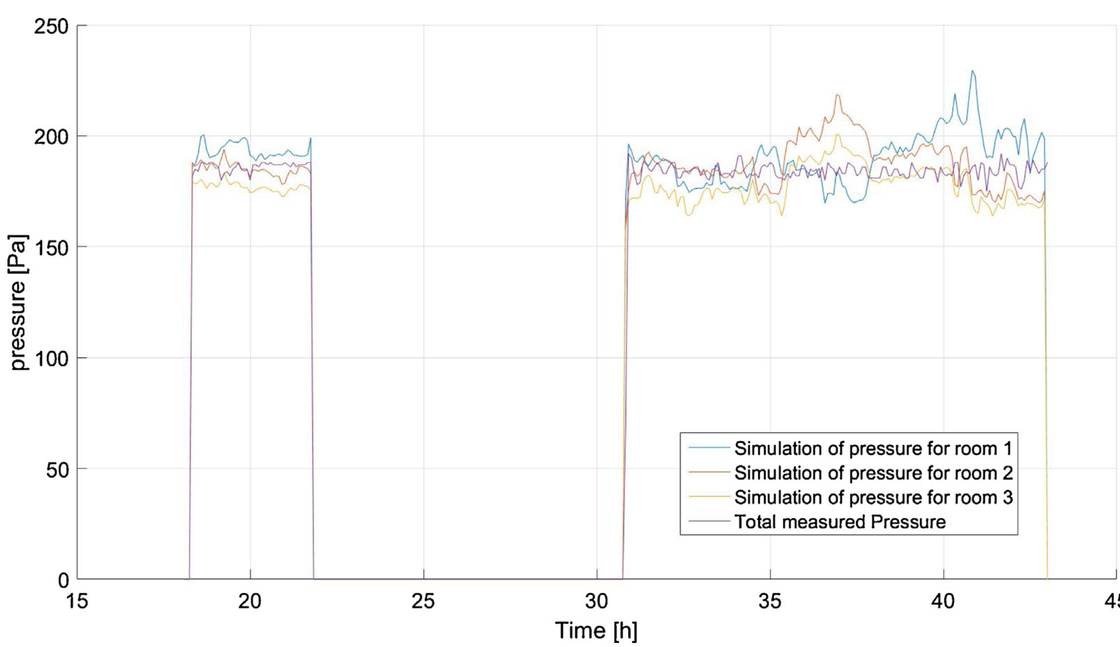

Fig. 8. Operation data of the pressure in the duct system.

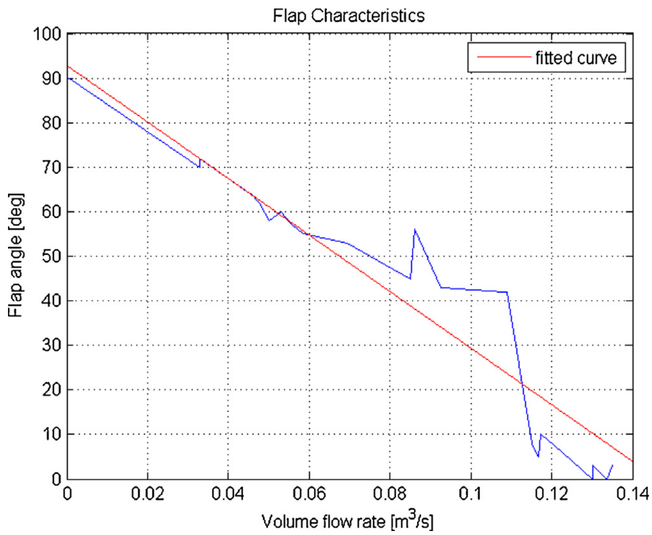

Fig. 9. Characterization of the VAV flap with regards to the flap angle and the volume flow rate.

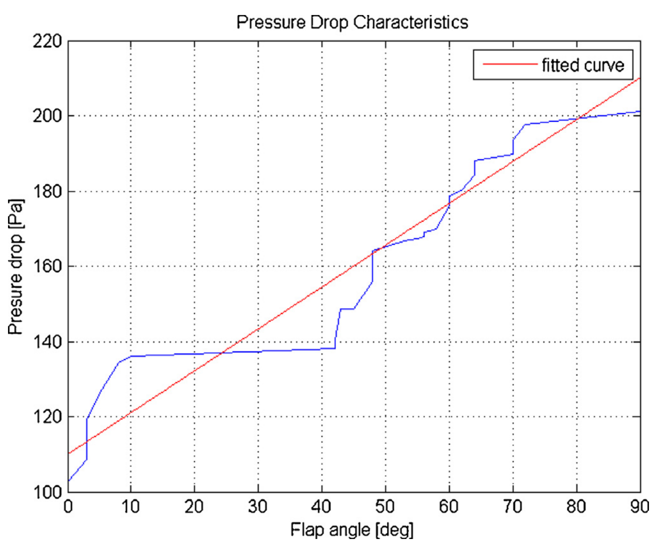

Fig. 10. Characterization of the VAV flap with regards to the pressure drop and the volume flow rate.

(flap) unit, the pressure drop across the VAV (flap) unit and the flap opening which is expressed in terms of an opening angle (in degrees, with 90° being fully closed). As only the volume flow rate is recorded by the building automation system, the parameters pressure drop and flap angle need to be calculated. For that reason a hybrid composition of a physical pressure drop model as shown in Section 4.1 and the available monitoring data served as the basis for the identification of the VAV's flaps.

Figs. 9 and 10 show the validation of the flap characteristics using the mathematical model and overlaying it with measurement data. Apart from the linear approximation, we also performed curve fitting using exponential functions and multiple order polynomials. However, these did not show any improvements compared to the linear fit. It is obvious that the measured data have a high ratio of noise, which is due to both dynamic effects of laminar air flow as well as design constraints of the duct system, which also explains e.g. the plateau in Fig. 10 between 10° and 40°. A further analysis of the dynamic effects would better explain the measured data, but would require additional effort in modeling and instrumentation. Therefore, a linear model was selected to approximate the characteristics and was therefore used for further processing. Using curve fitting algorithms led to the following linear equations:

$$\alpha = -634.6 * \dot{V} + 92.88 \quad (15)$$

$$\Delta p = 1.112 * \alpha + 109.9 \quad (16)$$

The linear approximation also allows the transformation of the above equation in case a flap angle is known at a certain pressure difference and the volume flow shall be validated. For volume flow rates that tend towards zero, logic is implemented to constrain Eq. (15) such that the angle is limited to 90°. The same is done for very high volume flow rates, meaning that the flap is fully open, therefore making $\alpha = 0°$.

This flap characteristic completes the pressure drop model of the duct topology and allows having a complete description of the controlled plant from the supply fan to the room outlet.

6.4. Comparison of ventilation controllers

Out of the different air quality controllers in Section 3 the authors have selected the Trim-and-Respond controller as a baseline for comparison with the controller presented here. It is more advanced than the Constant Static Pressure (CSP) and thus provides a fair baseline for the work in this paper. The Trim-and-Respond reduces air pressure until the first VAV controller has an opening angle of 90%; this is the trigger to increase the pressure again to prevent under-supply. As stated earlier, rapid changes of the IACQ are compensated only with a delay before the requested volume flow is provided. The comparison of the Trim-and-Respond controller and the new controller described in Section 5 had to be done in a simulated setup in order to eliminate the disturbances described earlier (leakages, occupancy, window air exchange rate), which would have provided results with high noise and potential biases. The noisy data result from the setup in an operational building and would require to collect a large sample of data to make statistically significant statements on the improvements, which again requires a tight integration into the building automation system that needs to be run in closed-loop operation with an (experimental) innovative controller. This could not be established within the scope of this work, therefore a simulation setup had to be chosen, which matches a section of the demonstration system described in Section 6.1. This setup consists of three rooms, as shown in Fig. 4, two offices (both of size $6 \times 4 \times 2.8$ m) and one conference room (size $4 \times 4 \times 2.8$ m). The maximum volume flow for air supply is designed to be 800 m^3/h, the occupancy profiles were selected to be constant during office hours with two people in the offices and five people in the conference room.

As shown in Fig. 11 the set-point of the CO_2 level (800 ppm) can be reached at about time t = 500 s (before that time there is no need for the controllers to act, since the CO_2 level is below the set-point) by both the baseline Trim-and-Respond controller and the controller developed in this work with about the same dynamics and accuracy. The CO_2 level of room 3 rises slower due to the relatively lower occupancy (i.e. less people per cubic meter air) and starts closing as soon as a volume flow in the duct system is recognized so that the overshoot is reduced (shown as a knee time t = 600 for room 1 and 2).

With regard to indoor air quality Fig. 12 shows that the newly developed controller reaches the comfort zone with comparable dynamics, but achieves this with lower power consumption: Fig. 12 shows the volume flow into the three rooms, indicating that Trim-and-Respond needs more volume flow while having about the same settling time. Additionally, the Trim-and-Respond controller requires a higher fan pressure. Therefore, the built-in flaps need to close much more to compensate the overpressure. This happens, because the Trim-and-Respond controller operates with a fixed

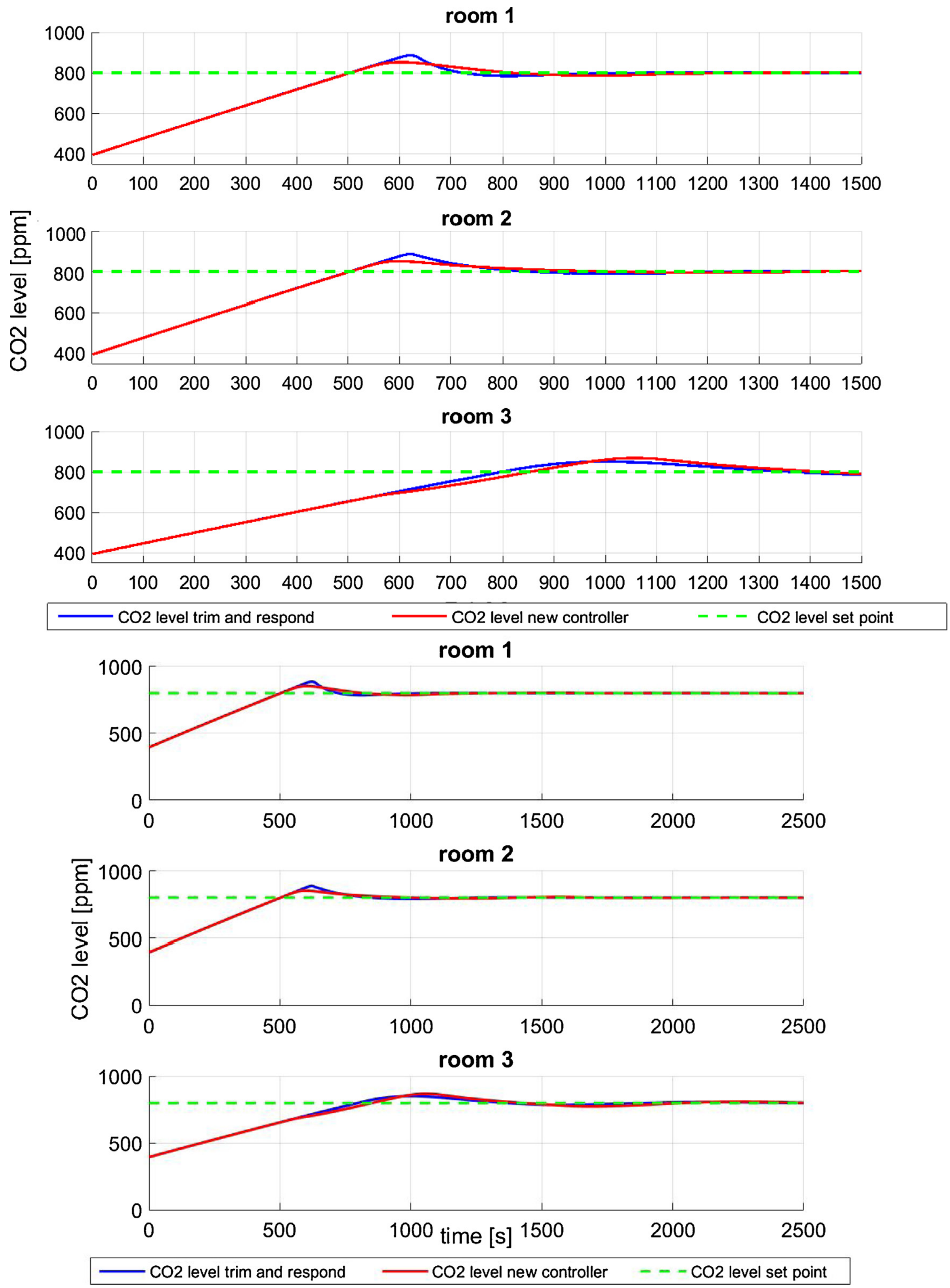

Fig. 11. CO_2 Level in three rooms.

pressure setting that is changed only after long time periods to avoid oscillations in the duct system. Only when the fan begins to lower the pressure the power consumption reduces. The newly developed controller, on the other side, communicates between the fan and the flaps immediately. Because of this improvement, the pressure can be kept quite low, so the power consumption is lower than by using the Trim-and-Respond controller and the system operates smoother.

Fig. 13 shows the differences in supply pressure between the two controllers, resulting from the volume flow demands of the three rooms that need to be provided by the supply fan. The new pressure controller for the supply fan is robustly designed, so that short-term changes do not affect and destabilize the system. Therefore, the controller reacts a bit slower than the Trim-and-Respond controller, but with a much lower pressure peek. Since both controllers maintain a similar level of air quality (Fig. 11) it is valid

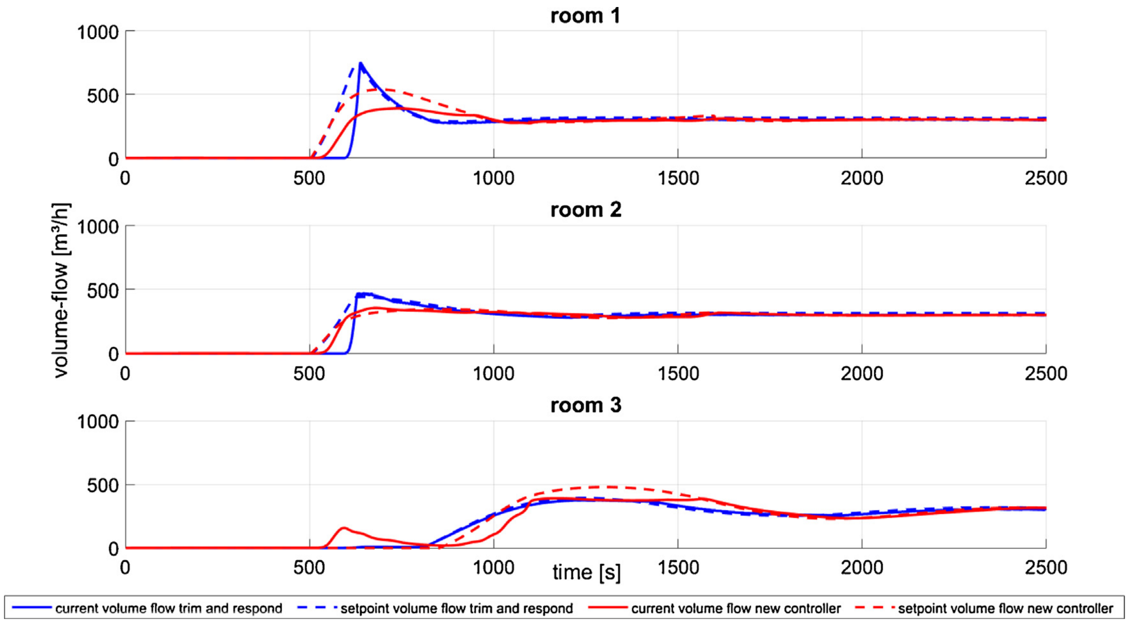

Fig. 12. Volume flow comparison in three rooms.

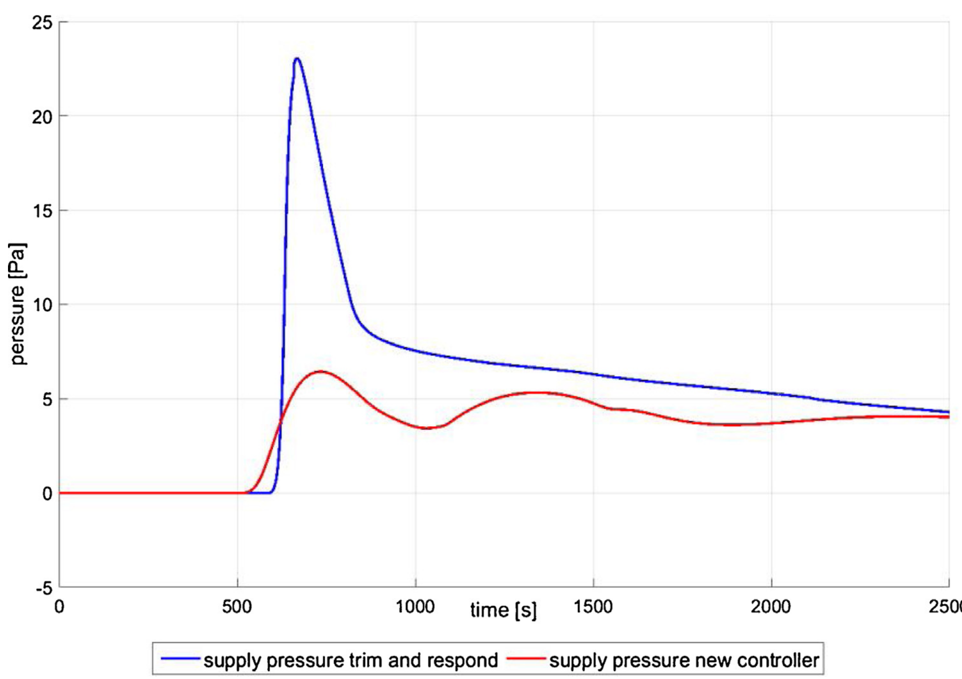

Fig. 13. Comparison of pressure difference.

to compare the energy saving potential of the new approach: by comparing the power consumption between the newly developed and the Trim-and-Respond controller an energy saving of about 5% could be identified due to the tighter link between volume flow and required supply fan pressure.

7. Conclusion and outlook

The work presented in this paper is driven by the idea of replacing hardware and investment costs with advanced algorithms that can be implemented in software. A dynamic pressure drop model for the duct ventilation system and its components was developed together with a controller that increases energy efficiency by coupling supply pressure and room volume flows more tightly. The controller is capable of operating either VAV boxes or motor flaps, it only requires the additional flap characteristics, which have been identified using operation data.

With regard to cost savings an estimate has been made for a reference office building: the building was built in 2015 according to passive house standard, has optimized daylight usage as well as concrete core activation with a gross floor area of 3100 m^2. The ventilation system uses a total of 100 VAV boxes of different sizes from size DN100 to the largest being 500 × 200 mm. Common market prices indicate investment cost saving from VAV controller to motor flap of 55%, which results in a total investment cost saving of about 11,000 EUR; other costs for operation and maintenance remain approximately the same. This defines the margin how much the additional controller software may cost per building; additionally the presented controller improves energy efficiency by another 5%, which can be significant, seeing that the ventilation system is one of the main energy consumers in a building.

The approach requires significant modeling effort, which is not feasible for practical implementation. Also, the validation of the controlled plant is difficult due to its multiple disturbances (including deviations from as-planned versus as-built system, mismatches in the flap model and the CO_2 room model). Although the controller is capable of compensating for these plant-model mismatches, since it operates in closed-loop, improvements need to be made. The main modeling effort affects the pressure drop model. Although there is some commercial software, it may be difficult to combine with some controller software, since the tools are mainly used for planning and not for operation.

A promising approach is grey box modeling, where the model is created by its topology and provided with the start values taken from literature as shown in this paper, but is calibrated with operation data in order to achieve an optimal plant-model fit. These obtained models can be used as local pressure drop models for each room/section in an office building. Thus, the determination of the highest pressure drop is possible and the ventilators pressure setpoint can be kept minimal. Thereby, the high modeling effort is reduced and different errors, like leakages, are compensated. This procedure can then be executed regularly in order to address aging, leaks or refurbishments.

Since the way of planning buildings is currently redefined using digital integrated planning by means of the Building Information Model (BIM), the modeling effort for duct system and components will potentially be reduced significantly, once this data is available from the planning phase and can directly be used in operation. This may go as far as extracting the ventilation system from a BIM and automatically deriving the optimal control strategy based on the topology and the indoor comfort parameters.

The BIM process has already penetrated the planning phase, but has not yet arrived in the operation phase; however, standardization activities are taking place, for example, in the Austrian Standards Committee 011.09 and it is expected that in the near future the necessary building data will be available for equipment operation.

Acknowledgement

This work is partly funded by the Austrian Research Promotion Agency (FFG) within project ARIS (grant agreement number 845143).

References

[1] D. Bosseboeuf, Energy Efficiency Trends and Policies in the Household and Tertiary Sectors – An Analysis Based on the ODYSSEE and MURE Databases, 2015.
[2] L. Pérez-Lombard, J. Ortiz, C. Pout, A review on buildings energy consumption information, Energy Build. 40 (3) (2008) 394–398.
[3] Commercial Buildings Energy Consumption Survey (CBECS) – U.S. Energy Information Administration (EIA). [Online]. Available: https://www.eia.gov/consumption/commercial/estimation-enduse-consumption.php (Accessed: 14-Jul-2017).
[4] M.F. Silva, S. Maas, H.A. de Souza, A.P. Gomes, Post-occupancy evaluation of residential buildings in Luxembourg with centralized and decentralized ventilation systems, focusing on indoor air quality (IAQ). Assessment by questionnaires and physical measurements, Energy Build. 148 (2017) 119–127.
[5] C.-A. Roulet, Santé et qualité de l'environnement intérieur dans les bâtiments, Presses Polytechniques et Univ. Romandes, Lausanne, 2004.
[6] Z. Lin, T.T. Chow, K.F. Fong, C.F. Tsang, Q. Wang, Comparison of performances of displacement and mixing ventilations. Part II: indoor air quality, Int. J. Refrig. 28 (2) (2005) 288–305.
[7] C.S. Koulani, C.A. Hviid, S. Terkildsen, Optimized damper control of pressure and airflow in ventilation systems, 10th Nordic Symposium on Building Physics (2014) 822–829.
[8] S.T. Taylor, Increasing efficiency with VAV system static pressure setpoint reset, ASHRAE J. 49 (6) (2007) 24.
[9] Standing Standard Project Committee (SSPC), ASHRAE Standard 62–2001, Ventilation for Acceptable Indoor Air Quality, 2001.
[10] Belimo, Belimo VAV compact, 05-Jul-2016. [Online]. Available: http://www.belimo.ch/pdf/d/LE_EU-CH_DE-CH_VAV-Compact.pdf [Accessed: 05-Jul-2016].
[11] X. Lin, J. Lau, Demand controlled ventilation for multiple zone HVAC systems: CO2-based dynamic reset (RP 1547), HVAC&R Res. 20 (8) (2014) 875–888.
[12] R.J. Garde, Fluid Mechanics Through Problems, New Age International, 1997.
[13] M.C. Potter, D.C. Wiggert, B.H. Ramadan, Mechanics of Fluids, si edition, Cengage Learning, 2016.
[14] W.-P. Sung, J.C.M. Kao, R. Chen, Frontiers of Energy and Environmental Engineering, CRC Press, 2012.
[15] D.I.H. Barr, H.W., (Firm), Tables for the Hydraulic Design of Pipes, Sewers and Channels Thomas Telford (2006).
[16] W.S. Janna, Design of Fluid Thermal Systems – SI Version, Cengage Learning, 2010.
[17] I.E. Idelchik, E. Fried, Handbook of Hydraulic Resistance, 1986.
[18] A.W.W. Association, B.E. Bosserman, A. Ali, I.M. Schuraytz, Butterfly Valves: Torque, Head Loss, and Cavitation Analysis, American Water Works Association, 2012.
[19] B.G. Liptak, Instrument Engineers' Handbook: Process Control, Vol. 2, Third Edition, CRC Press, 1995.
[20] Fenster und Türen -Luftdurchlässigkeit -Klassifizierung. DIN EN 12207, (2000).
[21] EnEV Anforderungen an die Dichtheit und den Mindestluftwechsel, 07-Jul-2015. [Online]. Available: http://www.enev-online.org/enev_2009_volltext/enev_2009_anlage_04_anforderungen_dichtheit_mindestluftwechsel.htm.
[22] A. Maas, Experimentelle Quantifizierung des Luftwechsels bei Fensterlüftung, Kassel.
[23] J. Burkhardt, Deutschland, Daten zur Umwelt: der Zustand der Umwelt in Deutschland. 7. 2000, E. Schmidt, Berlin, 2001.
[24] N. US Department of Commerce, ESRL Global Monitoring Division – Global Greenhouse Gas Reference Network. [Online] Available: https://www.esrl.noaa.gov/gmd/ccgg/trends/global.html [(Accessed: 07-Feb-2017).
[25] Ausschuss für Umwelthygiene, Standards zur Expositionsabschätzung Hamburg, 1995.